here indicate a coefficient between $\frac{2}{3}$ and 1, at the present there is no theoretical justification for such a number.

CONCLUSIONS

From the work reported above, it was concluded that the self-consistent APW method of calculating the energy-band structure of metallic copper yields results that are in reasonably good agreement with experimental results. It was also concluded that the agreement could be improved if a self-consistent APW calculation were carried out in which the exchange was reduced to a fraction somewhere between 1 and $\frac{2}{3}$ of the Slater free-electron approximation.

ACKNOWLEDGMENTS

The authors wish to thank Dr. A. C. Switendick for his considerable help and guidance during all stages of this work. Without his counsel, and without the computer programs which he and Dr. J. H. Wood made available to us, completion of this research would have been considerably delayed. The kind interest and assistance of F. W. Schonfeld and W. N. Miner were also appreciated.

PHYSICAL REVIEW VOLUME 157, NUMBER 3 15 MAY 1967

Effect of Sample Geometry on Magnetomorphic Oscillations in the Hall Effect in Cadmium at Liquid-Helium Temperatures

H. J. MACKEY, J. R. SYBERT, AND J. T. FIELDER
Department of Physics, North Texas State University, Denton, Texas
(Received 19 December 1966)

Size-effect oscillations in the Hall resistivity have been studied in a monocrystal of highly pure cadmium at liquid-helium temperatures. Samples ranging in thickness from 2.01 to 0.09 mm were prepared from a single monocrystal by successively reducing the thickness using spark planing followed by electropolishing. The probes were not removed during this process to ensure that the samples were representative of a common background of orientation, strain, purity, and surface condition. The magnetic field was applied parallel to the hexagonal axis, and dependence on thickness parallel to this direction was studied in the period, phase, and amplitude of the oscillations. The amplitude was observed to increase as thickness was reduced. The oscillations are not strictly periodic, but the apparent period is proportional to the reciprocal thickness. The phase of the oscillations is determined to be zero, although existing theory predicts a phase of $\pi/2$. It is concluded that the lens-shaped pocket of electrons in the third Brillouin zone is responsible for the oscillations. The radius of curvature of the lens apex in the hexagonal direction is determined to be $k_F = 1.37$ Å^{-1}. A study of the temperature dependence of the amplitude of the oscillations implies that the mean free path is in the millimeter range at liquid-helium temperatures. A careful search for short-period oscillations observed by other researchers was fruitless. Data from an electropolished sample were compared to those from a spark-planed sample of the same dimensions; the amplitude of the oscillations was found to be twice as large in the spark-planed sample data as in the electropolished sample data. A slight increase in amplitude was effected by abrading an electropolished sample with No. 600 SiC paper. This enhancement in amplitude implies that an appreciable number of electrons scatter specularly at the electropolished surfaces. It is suggested that a very thin distorted layer at the crystal surface may be necessary to observation of the short-period oscillations.

INTRODUCTION

IN thin metal plates or wires where the mean free path is comparable to or greater than the dimensions of the sample, one must consider the effects of boundary scattering in problems of electron transport. The phenomena introduced by boundary scattering are known as size or morphic effects. The problem of increased resistivity in thin films was first considered as early as 1901 by Thomson.[1] Following that initial attempt, several contributions to the theory have appeared[2–5] and, in recent years, various experiments related to the size-effect phenomena have been reported. Much of this work relates to the case of either longitudinal magnetic fields or zero magnetic field.[6] Sondheimer[7] has treated the case of conductivity in thin samples with a transverse magnetic field. In particular, he predicted oscillations in the Hall effect and transverse magnetoresistance as a function of magnetic field with the magnetic field applied perpendicular to the plane of a thin con-

[1] J. J. Thomson, Proc. Cambridge Phil. Soc. **11**, 20 (1901).
[2] A. C. B. Lovell, Proc. Roy. Soc. (London) **A157**, 311 (1963).
[3] K. Fuchs, Proc. Cambridge Phil. Soc. **34**, 100 (1938).
[4] L. Nordheim, Act. Sci. Ind. No. **131**, (1934).
[5] D. K. C. MacDonald and K. Sarginson, Nature **164**, 921 (1949).
[6] See Ref. 19 for an extensive bibliography.
[7] E. H. Sondheimer, Phys. Rev. **80**, 401 (1950); Advan. Phys. **1**, 1 (1952).

ducting plate.[8] A limited number of experiments have been reported confirming these oscillatory effects both in single crystals and in polycrystalline materials.[9–17] Blatt has extended the Sondheimer theory to include magnetothermal effects.[18] Recently, magnetomorphic oscillations have been observed in transport effects other than the electrical conducitivity.[19]

In this paper we report observations on size-effect oscillations in the Hall effect in an oriented single crystal of highly pure cadmium at liquid-helium temperatures. All measurements were made in a transverse magnetic field (see Fig. 1). Size-effect data for different thicknesses of the same crystal were obtained in order to gain an absolute indication of the effect of this parameter on the amplitude, phase, period, and damping of the oscillations. The effect of surface damage is examined, and a case is made for the existence of specular reflection from a surface with irregularities many times larger than the de Broglie wavelength of the impinging electrons. The variation of mean free path with temperature is examined for temperatures in the liquid-helium range. Finally, the results are analyzed in terms of a previously proposed model for the portion of the Fermi surface responsible for the effect.[20]

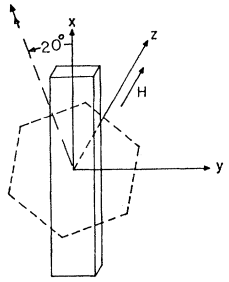

FIG. 1. Crystal orientation with respect to applied magnetic field **H** and crystal symmetry axes. The hexagonal axis is along the z axis and parallel to **H**, with the binary axis in the x-y plane tilted 20° from the x axis. Electric current is in the positive x direction, and the Hall probes sample the electric field in the y direction.

THEORY

The Sondheimer Model

Sondheimer[7] has calculated the conductivity tensor for the case of an infinite, isotropic, crystalline film with a magnetic field perpendicular to the plane of the film. Assuming a spherical Fermi surface, diffuse reflection at the crystal boundaries, and the existence of a relaxation time, the Boltzmann equation is solved for the perturbation to the equilibrium Fermi distribution. The presence of the limiting surfaces, $z=0$, a, is taken into account by requiring the perturbation f_1 to go to zero at $z=0$, a. The results of this calculation are summarized below in order to compare the resulting expressions with those one may derive from a very naive kinetic picture of the mean electronic motion. Sondheimer finds

$$f=f_0+f_1=f_0+(v_xc_1+v_yc_2)\partial f_0/\partial v\,, \tag{1a}$$

$$c_1-ic_2=e\tau E/mv[1+(ieH\tau)/mc]$$
$$\times[1+h(\mathrm{v})\exp\{-(1+ieH\tau/mc)z/v_z\tau\}]\,, \tag{1b}$$

where

$$h(\mathrm{v})=-1 \qquad \text{for } v_z>0. \tag{1c}$$

$$h(\mathrm{v})=-\exp\{[1+(ieH\tau)/mc](a/v_z\tau)\} \quad \text{for } v_z<0. \tag{1d}$$

The complex electric field is $E=E_x-iE_y$, and **H** $=(0,0,H)$ is the magnetic field. Defining a complex current density, $J=J_x-iJ_y$, one obtains

$$dJ(v_z)=dn(v_z)(e^2\tau'/m)$$
$$\times\{1+[v_z\tau'/a][\exp(-a/v_z\tau')-1]\}E\,, \tag{2}$$

where $dJ(v_z)$ is the average, over the thickness of the crystal, of the contribution of the electrons $dn(v_z)$ belonging to a slice of the Fermi sphere bounded by the planes v_z, v_z+dv_z.

The quantity τ' is defined by $1/\tau'=(1/\tau)+i(eH)/mc)$. Defining

$$t=v_F/v_z, \quad \lambda=v_F\tau, \quad H_0=mv_Fc/ea\,,$$
$$s=(a/\lambda)+i(H/H_0)=\kappa+i\beta\,, \tag{3}$$
$$J_x-iJ_y=(\sigma_{11}+i\sigma_{12})(E_x-iE_y)\,,$$

and integrating (2) over the Fermi sphere, one obtains the result

$$\sigma_{11}+i\sigma_{12}=\tfrac{3}{2}\sigma_b\int_1^\infty (t^{-2}-t^{-4})$$
$$\times\{1+(st)^{-1}[\exp(-st)-1]\}dt\,, \tag{4}$$

where the bulk conductivity is

$$\sigma_b=nec(H_i-iH)/(H^2+H_i^2)\,, \tag{5a}$$

and the saturation field is

$$H_i=mc/e\tau. \tag{5b}$$

Grenier[19] has shown that if one picks out the oscillatory term in Eq. (4) and expands by integration by parts, the first term gives a good approximation for the

[8] Actually Sondheimer's final analytical result is our Eq. (4), and he has demonstrated the oscillations in σ_{11} by numerical integration of this equation. However, the integration was not carried out for large enough values of β in the case of σ_{12}, and the oscillations were not exhibited. See Ref. 13, Fig. 1, for the results of an extended integration of Eq. (4).

[9] D. K. C. MacDonald, Nature **163**, 637 (1949).

[10] E. R. Andrew, Proc. Phys. Soc. (London) **62**, 77 (1949).

[11] J. Babiskin and P. H. Siebenmann, Phys. Rev. **107**, 1249 (1957).

[12] M. Yaqub and J. F. Cochran, Phys. Rev. Letters **10**, 390 (1963); Phys. Rev. **137**, A1182 (1965).

[13] N. H. Zebouni, R. E. Hamburg, and H. J. Mackey, Phys. Rev. Letters **11**, 260 (1963).

[14] J. M. Reyonlds, K. R. Efferson, C. G. Grenier, and N. H. Zebouni, in *Proceedings of Ninth International Conference on Low Temperature Physics, Ohio State University, 1964* (Plenum Press, Inc., New York, 1965), p. 808.

[15] J. A. Munarin and J. A. Marcus, in *Proceedings of Ninth International Conference on Low Temperature Physics, Ohio State University, 1964* (Plenum Press, Inc., New York, 1965), p. 743.

[16] K. R. Efferson, C. G. Grenier, and J. M. Reynolds, Bull. Am. Phys. Soc. **10**, 126 (1965).

[17] K. Førsvall and I. Holwech, Phys. Letters **3**, 66 (1962).

[18] F. J. Blatt, Phys. Rev. **95**, 13 (1954).

[19] C. G. Grenier, K. R. Efferson, and J. M. Reynolds, Phys. Rev. **143**, 406 (1966).

[20] M. R. Daniel and L. MacKinnon, Phil. Mag. **8**, 537 (1963).

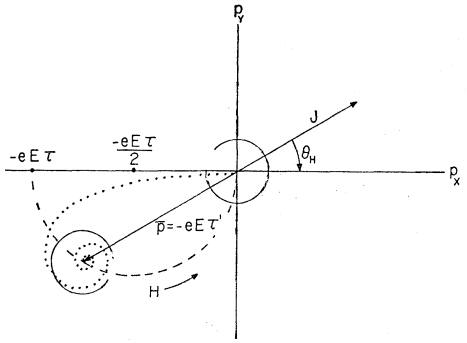

FIG. 2. The transient motion of the Fermi sphere in a viscous medium under the influence of crossed electric and magnetic fields. The electric field is along the x direction, and the magnetic field is along the z direction. The curved arrow labeled H indicates the motion of the steady-state momentum $\bar{p}$ along the dashed semicircle as H is increased. The radius of the Fermi sphere is many orders of magnitude larger than $eE\tau$, but has been reduced for clarity. The dotted spiral indicates the transient motion of the center of the Fermi sphere.

high magnetic-field oscillatory phenomena. One finds

$$\tilde{\sigma}_{11}+i\tilde{\sigma}_{12}=(\pm 3\,|\sigma_{12_b}|\beta^{-3}e^{-\kappa})\times[\cos\beta+i\,\cos(\beta+\pi/2)], \quad (6)$$

where the upper sign refers to a sphere of electrons, and the lower sign refers to a sphere of holes.

A. Kinetic Model

It is interesting to note that one may derive precisely the foregoing results from a simple kinetic model which gives physical insight into the nature of the ocsillations.

Consider an electron at rest in a viscous medium. At $t=0$, switch on crossed electric and magnetic fields, $\mathbf{E}=(E,0,0)$, $\mathbf{H}=(0,0,H)$. The equation of motion is

$$d\mathbf{p}/dt=-e\mathbf{E}-(e/mc)\mathbf{p}\times\mathbf{H}-\mathbf{p}/\tau. \quad (7)$$

The solution to Eq. (7), written in complex notation, is

$$p=eE\tau'[\exp(-t/\tau')-1], \quad (8a)$$

where

$$p=p_x+ip_y, \quad (8b)$$

and

$$1/\tau'=1/\tau-i(eH/mc). \quad (8c)$$

Figure 2 indicates that the trajectory in momentum space is a decaying spiral to the point $\bar{p}=-eE\tau'$ which lies on a semicircle passing through the origin and centered at the point $-eE\tau/2$. Note that the Hall angle approaches $-\pi/2$ for $H\gg H_i$. Solution for electrons possessing initial momentum shows similar decay to the same point $\bar{p}$; however, the exclusion principle forces the sphere to move rigidly and center on $\bar{p}$. Then Eq. (8) gives the gain in momentum for every electron in the sphere.

Now assume the crystal is limited in the z direction by the planes $z=0$, a. Diffuse scattering at these planes implies that on collision the average electron reverts to its initial position in the equilibrium sphere centered on the origin. Consider electrons belonging to a slice of the sphere bounded by planes v_z, v_z+dv_z, for $v_z>0$. On arriving at an element of crystal in the range z, $z+dz$, these electrons have been on their spiraling paths for time $t=z/v_z$ since scattering from the lower surface. Then from Eq. (8) their gain in momentum is

$$\Delta p_+=eE\tau'[\exp(-z/v_z\tau')-1]. \quad (9)$$

Giving the same consideration to the conjugate slice of sphere for $v_z<0$, one obtains

$$\Delta p_-=eE\tau'\{\exp[(z-a)/v_z\tau']-1\}. \quad (10)$$

The contribution of these slices to the current density at z is essentially

$$dJ(z,v_z)=-dn(v_z)e\Delta p_+/m, \quad (11)$$

where $dn(z,v_z)$ is the number of electrons per unit volume belonging to both slices. Substitution of Eq. (9) into Eq. (11) gives

$$dJ(z,v_z)=[dn(v_z)e^2\tau'/m][1-\exp(-z/v_z\tau')]E. \quad (12)$$

One may now average Eq. (12) over the thickness to obtain

$$dJ(v_z)=[dn(v_z)e^2\tau'/m]\{1+(v_z\tau'/a)\times[\exp(-a/v_z\tau')-1]\}E. \quad (13)$$

Taking the complex conjugate of Eq. (13) yields the Sondheimer result, Eq. (2), by virtue of the definitions given in Eqs. (3) and (8). The similarity between the exponentials appearing in Eq. (1) and those in Eqs. (9) and (10) is obvious.

This viscous-medium model shows that the average motion of an electron is a rapid, decaying spiral superimposed on a small constant drift in the x-y plane, plus a rapid constant motion in the z direction. As the magnetic field is increased, the pitch of the helix decreases. Maxima in $\tilde{\sigma}_{11}$ should occur whenever the pitch is such that an integral number of turns are executed during the transit between surfaces. Maxima in $\tilde{\sigma}_{12}$ should occur for $(n-\frac{1}{4})$ turns, where n is an integer. (The symbols $\tilde{\sigma}_{12}$ and $\tilde{\sigma}_{11}$ denote the oscillatory components of the Hall conductivity σ_{12} and the magnetoconductivity σ_{11}, respectively.)

Consider a sample which has a distorted or strained layer of depth d at one surface. Then when the associated integer rises to $n\approx a/d$, such that one or more turns of the helix spans the distorted layer, it may be expected that a significant proportion of the electrons act as if the thickness were reduced by d, and the resulting superposition of maxima and minima will lead to damping of the observed oscillations. A similar argument applies to the case of surfaces which are somewhat rounded, i.e., damping will occur when the pitch of the helix is of the order of the deviation from perfect geometry.

Grenier[19] has extended the Sondheimer theory to the case of Fermi surfaces which are axially symmetric about the z axis. In particular a lens-shaped pocket of the form which occurs in the third Brillouin zone in cadmium has been considered. The essential differences in the results of these calculations as compared to Eq. (6) are a reduction in the predicted amplitude of the oscillations by a factor of 0.58 and the substitution of the radius of curvature of the lens apex for the radius of the Fermi sphere which reduces the expected period by a factor of 0.97. No change in phase is found. The following discussion is based on Grenier's formula, Eq. (6), but the kinetic-model terminology will be convenient. It should be pointed out that Gurevich[21] has considered very general Fermi surfaces, and the essential result is that the Gaussian curvature of the surface is introduced.

The oscillations $\tilde{\sigma}_{12}$ are attributed the following properties by Eq. (6):

(1) period $=P_0=2\pi H_0=2\pi m v_F c/ea$,

(2) maxima should occur when $H=H_n=(n-\delta/2\pi)P_0$, with $\delta=\pi/2$ and n an integer,

(3) the amplitude should decay as H^{-4} at high field,

(4) at constant H, the amplitude should vary with temperature as $e^{-a/\lambda(T)}$.

It is more convenient to consider these properties in terms of the oscillatory component of the Hall resistivity $\tilde{\rho}_{21}$. Since the magnetoresistance ρ_{11} is two orders of magnitude greater than ρ_{21} in cadmium and increases quadratically with magnetic field, one finds for large magnetic fields

$$\rho_{11}=\alpha H^2, \tag{14a}$$

$$\tilde{\rho}_{21}=(\rho_{11})^2\tilde{\sigma}_{12}=\alpha^2 H^4\tilde{\sigma}_{12}. \tag{14b}$$

The oscillatory part of ρ_{11} is of the same order as $\tilde{\rho}_{21}$ and is entirely negligible compared to the gross ρ_{11}. Equation (14) implies that $\tilde{\rho}_{21}$ has the same properties as $\tilde{\sigma}_{12}$ except that it should have constant amplitude at high magnetic field.

EXPERIMENTAL PROCEDURE

In order to test the Sondheimer theory in detail, it was considered important to measure the oscillatory phenomena in a group of single crystals representing a range in dimensions from matchbox geometry to thin-film geometry, and to obtain samples identical with respect to impurity content, strain, orientation, surface condition, and probe placement. This was accomplished by the successive thinning of a single sample without removing the probes.

The initial single crystal was spark machined from an ingot of 69-grade cadmium obtained from Cominco Products, Inc., Spokane, Washington. It was x-ray oriented and spark machined into parallelepiped geometry of dimensions 27.0×6.5×4.2 mm. The hexagonal axis was perpendicular to the large faces to within 1°, with the binary axis 20° from the longitudinal axis of the sample (see Fig. 1). The large faces were spark planed parallel to within 1°. In order to obtain a surface free of the polycrystalline layer produced by spark planing, the large faces were electropolished until approximately 100 μ were removed from each surface.

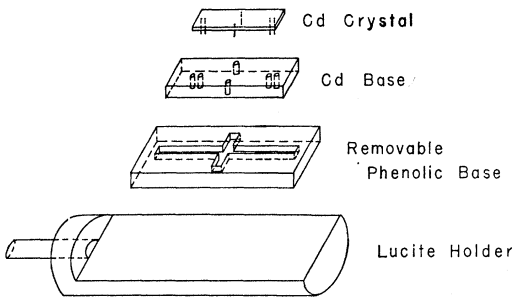

FIG. 3. The crystal assembly. The sample, cadmium base, and phenolic base form a unit which is removed intact from the Lucite holder for successive spark planing and electropolishing of the exposed face of the cadmium sample.

The electropolishing solution consisted of 57 cc of H_3PO_4 (specific gravity 1.689) in 43 cc of H_2O. A copper cathode was used. Experiment showed cathode geometry and placement had negligible effect; however, it was necessary to arrange the surface to be polished in the horizontal facing the liquid surface to avoid flow lines on the crystal produced by motion of the viscous film created under polishing conditions. Miccroshield[22] was used to isolate the other surfaces from the electrolyte. Polishing was carried out in a 250-ml beaker with a rectangular cathode set vertically at one side of the beaker. The cell was operated in the range 1.8 to 2.0 V with a current density of 42 mA/cm^2 establishing a removeal rate of 80 μ/h. Mirror finishes were easily obtained.

Current, magnetoresistance, and Hall probes were soldered to one polished face. To facilitate subsequent spark planing and electropolishing, the crystal was cemented rigidly to a cadmium base, probes side down. A thin coat of Miccroshield and a single sheet of cigarette paper were used to effect electrical isolation from the base. The cadmium base was used as a precaution against thermal strain associated with repeated cycling between room temperature and helium temperatures. Finally, the cadmium base was cemented to a phenolic base to form a rigid unit. Trenches were milled into the phenolic to provide an exit for the twisted probe leads (see Fig. 3). This unit could be conveniently mounted in the spark machine for further planing, and was small enough to fit in the electropolishing cell for further polishing.

External leads were brought into the Dewar system via an epoxy-sealed, thin-walled stainless-steel tube,

[21] V. L. Gurevich, Zh. Eksperim. i Teor. Fiz. 35, 668 (1958) [English transl.: Soviet Phys.—JETP 8, 464 (1959)].

[22] A polyvinyl chloride based blanking lacquer manufactured by Michigan Chrome and Chemical Company, Detroit, Michigan.

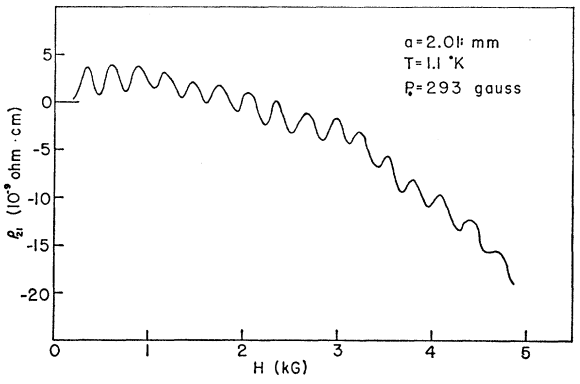

FIG. 4. The Hall resistivity ρ_{21} plotted as a function of magnetic field H. The oscillations, roughly periodic in magnetic field, are seen superimposed upon the nonoscillatory contribution. The general behavior of ρ_{21} with H for the thickest sample is typical of data obtained for various thicknesses of the sample.

fitted with a Lucite support table. The phenolic base was attached to the Lucite, and the short probe leads were soldered to the external leads prior to data runs. Care was taken to ensure that the helium level remained above all solder joins to prevent thermal emf's during the experiments.

After each experiment the leads were unsoldered and the phenolic detached from the Lucite table. Laue pictures were taken to ensure absence of strain. The sample

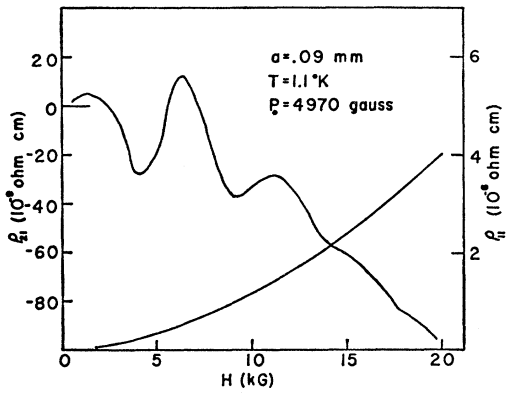

FIG. 5. Transverse magnetoresistivity ρ_{11} and Hall resistivity ρ_{21} for the 90-μ plate thickness. The Hall resistivity ρ_{21} shows the size-effect oscillations on the monotonic effect. The transverse magnetoresistance ρ_{11} is approximately quadratic in H and is used to relate ρ_{21} to the Hall conductivity σ_{12}. See Eq. (14).

was then planed and electropolished to smaller thickness. The final sample was not spark machined but was thinned by electropolishing only. This sequence produced surfaces which were quite plane-parallel except in the two thinnest samples. When the sample became quite thin, the current distribution about the edges caused significant rounding, resulting in a lens-shaped cross section.

The samples were examined with a Unitron Depthscope equipped with x-y translation drums calibrated directly in microns, and z translation calibrated to 5 μ. The experimental data curves are labeled by crystal thickness taking into account the 1.5% c-axis contraction at helium temperatures.[20] The values $a=0.16$ mm and $a=0.09$ mm are mean thicknesses corresponding to the lens-shaped cross section described above.

The potentials were measured by recording the offbalance of a Honeywell Six-Dial Thermal-Free Potentiometer, amplified by a Beckman Model 14 Breaker Amplifier. Data were taken for normal and reverse directions of the magnetic field, and the results were appropriately averaged to eliminate the effects of probe misalignment.

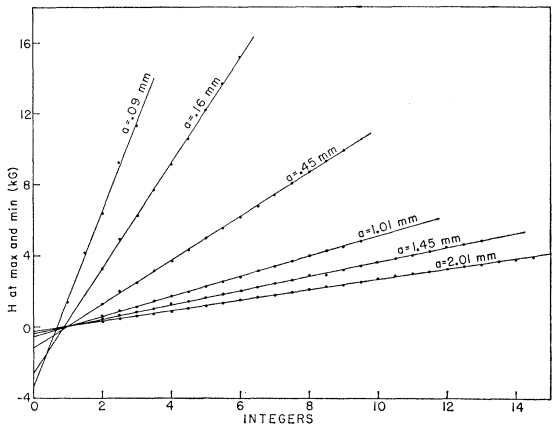

FIG. 6. Magnetic field positions of the maxima and minima of the oscillations in ρ_{21} plotted against integers. This is a period and phase plot for magnetomorphic oscillations corresponding to the various thicknesses of the monocrystal. The maximum in a given oscillation occurring nearest zero magnetic field is labeled $n=1$. The periods determined from the slopes are shown in Fig. 7. The oscillations are not strictly periodic, but a large number of maxima have been observed in order to obtain an accurate value of the average period.

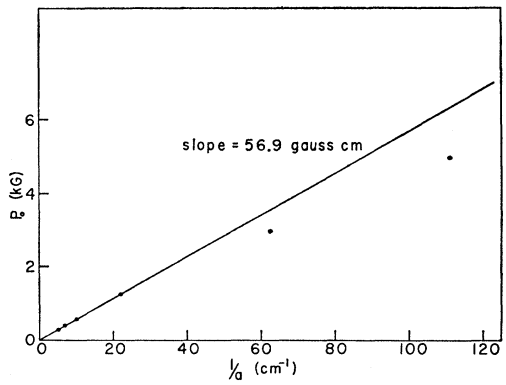

FIG. 7. Period of the size-effect oscillations in ρ_{21} plotted against reciprocal thickness for the various values of sample thickness. The period P_0 is strictly proportional to $1/a$ for the thicker samples with anomalous behavior for the very thin cases. The deviation from strict proportionality to $1/a$ in the thin samples is due to nonplanar surfaces.

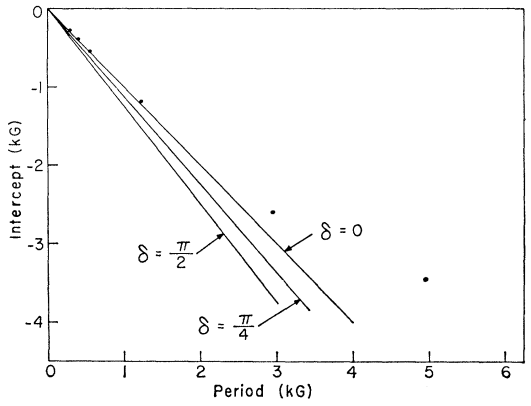

FIG. 8. Intercept plotted against period P_0 determined from the data shown in Fig. 6. The slopes of the straight lines correspond to three different values of the absolute phase δ. Theory predicts $\delta=\pi/2$, but it is seen that the experimental data for the four thickest cases indicate $\delta=0$ within 5%. The deviations from the line $\delta=0$ for the two points corresponding to the thinnest samples is due to nonplanar geometry.

RESULTS AND DISCUSSION

Comparison to Theory

The general behavior of ρ_{21} as thickness is reduced is indicated by the data for the thickest and thinnest samples shown in Figs. 4 and 5, respectively. The quadratic nature of ρ_{11} is to be noted in Fig. 5. An increase in

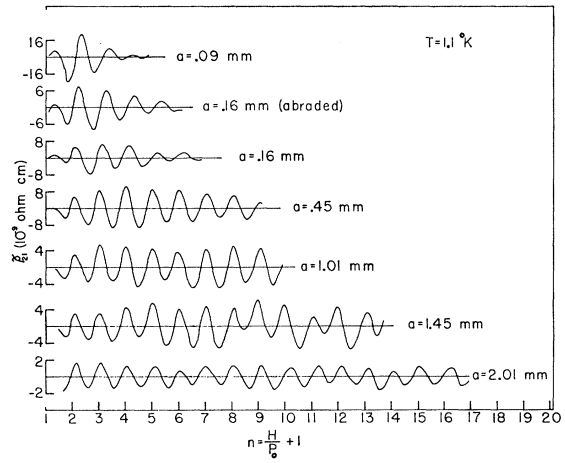

FIG. 9. A normalized plot of the oscillatory component $\tilde{\rho}_{21}$ of the Hall resistivity as a function of magnetic field H. The abcissa for each curve has been scaled using the values of P_0 corresponding to the specific thicknesses a. Since oscillation maxima occur for H an integral multiple of P_0, each curve appears to have the same frequency. Note that $n=1$ corresponds to a maximum for $H=0$.

period and amplitude is found as the thickness is decreased.

Equations (6) and (14) show that the field values at which $\tilde{\rho}_{21}$ is a maximum should occur for

$$H_{\max}=(n-\delta/2\pi)P_0. \tag{15}$$

Thus a plot of $H_{\max}$ versus n should yield a straight line of slope P_0. Figure 6 exhibits these data for the range of samples studied. The data are well represented by straight lines, and the slope is seen to increase with decreasing thickness. It should be noted that, with the exception of the thinnest samples, all the lines intersect the $H=0$ axis at $n=1$. The anomalous behavior of the thinnest samples will be discussed below.

Equation (6) implies that P_0 versus $1/a$ should be a straight line through the origin whose slope is $2\pi m v_F c/e$.

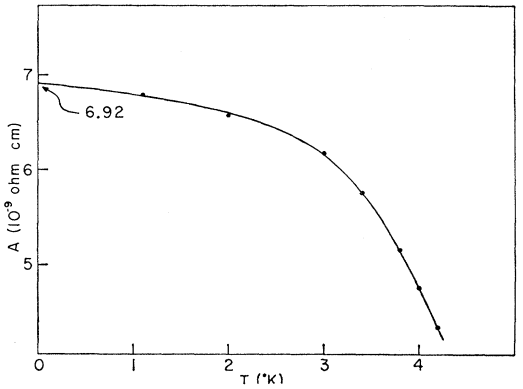

FIG. 10. Amplitude of the magnetomorphic oscillation in ρ_{21} plotted as a function of temperature. The data points are obtained in the vicinity of the third maxima ($n=3$) of the 0.16-mm sample. A smooth curve is drawn through the points, and the extrapolated value of $A=6.92\times10^{-9}$ Ω-cm at $T=0$°K is used in the calculation of the mean free path exhibited in Fig. 11.

This behavior is exhibited in Fig. 7. The data are seen to be well represented by such a line, again with the two thinnest samples anomalous. This line has slope 56.9 G cm corresponding to $p_F=1.45\times10^{-19}$ cgs or $k_F=p_F\hbar^{-1}=1.37$ Å^{-1}. These values are 2.8% smaller than those given by free-electron theory (1.41 Å^{-1}) for liquid-helium temperature. The lens-shaped pocket of electrons in the third zone is believed to be responsible for

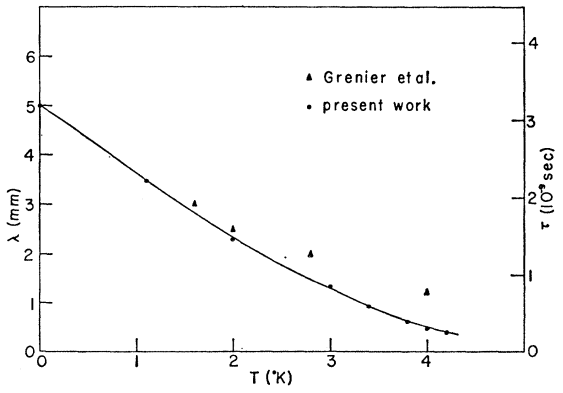

FIG. 11. Calculated values of electron mean free path as a function of temperature. The value of λ at $T=0$°K is obtained by extrapolation of the data of Grenier *et al.* (Ref. 18). The calculated values exhibit similar temperature dependence to those of Grenier *et al.* A scale for relaxation time τ is constructed using the value $v_F=1.58\times10^8$ cm/sec (Ref. 19).

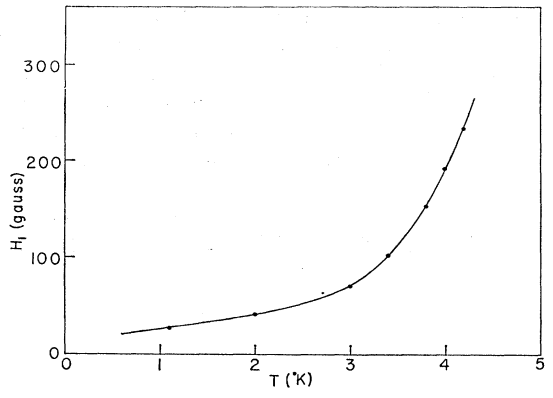

FIG. 12. Temperature dependence of the saturation field H_i [see Eq. (5)] for the lens-shaped pocket of electrons.

these oscillations. Using the principal axis radial values found by Daniel and MacKinnan,[20] one finds the radius of curvature of the lens apex is 1.36 Å^{-1}, which is 3.5% smaller than the radius of the Fermi sphere.[19] Thus the experimentally determined radius of curvature agrees with that expected from the lens geometry to within less than 1.0%.

Equation (15) shows that a plot of the intercept on the $H_{\max}$ axis I against P_0 should be a straight line through the origin whose slope determines the phase δ. The lines in Fig. 6 were obtained by a least-squares fit of the data. The intercepts thus obtained are plotted against P_0 in Fig. 8. It is seen that the data points fall well on the $\delta=0$ line, again with the exception of the two thinnest samples. Thus, theory predicting $\delta=\pi/2$ appears to be in error on this point. However, consider Fig. 9. This figure presents the $\tilde{\rho}_{21}$ directly, plotted in a normalized form. For δ strictly equal to zero, the maxima must all fall precisely at the integers, but examination of the figure shows the oscillations are not strictly periodic for any sample. The intercepts determined by least squares represent an average value for δ. However, it would be extremely fortuitous to obtain the data of Fig. 8 if δ deviates substantially from zero.

Figure 9 shows that the amplitude of $\tilde{\rho}_{21}$ is reasonably constant except in the two thinnest samples. This constancy validates the H^{-4} dependency of $\tilde{\sigma}_{12}$ predicted by Eq. (6).

The Effect of Abrasion and Imperfect Geometry

It was considered important to compare data taken on a single sample in the electropolished and in an abraded condition. Unfortunately, this was done on the 0.16-mm sample before its departure from parallel geometry was discovered. The exposed electropolished surface was abraded with No. 600 SiC abrasive paper held on a tuft of cotton to avoid pressure strains. The results are indicated in Fig. 9. A slight but definite increase in amplitude was observed for the abraded sample relative to the electropolished sample. Note that the abraded 0.16-mm sample shows a more rapid damping than the unabraded sample. This increase in damping is believed associated with the distorted surface layer introduced by abrasion. The damping already present in the 0.16-mm unabraded sample and that shown in the 0.09-mm sample is due to the departure from plane geometry. Note that the damping becomes appreciable in this sample at $n\approx 5$, implying the variation in thickness is on the order of 20%. The 0.16-mm label represents the mean thickness as determined by optical methods. It is significant that a thickness of $a=0.20$ mm is the effective thickness of the crystal needed to put its associated data point on the straight line in Fig. 7; i.e., the mean thickness is 20% less than the effective thickness. Similarly, the effective thickness of the thinnest sample is 0.12 mm implying significant damping for $n\approx 3$. This effect is seen clearly in Fig. 9. The anomalous behavior of the thinnest samples with respect to phase is to be expected due to the superposition of sinusoids of different periods occurring because of the nonplanar condition of the crystal faces.

Temperature Dependence

Equations (6) and (14) show that $\tilde{\rho}_{21}$ is proportional to $\exp[-a/\lambda(T)]$. The amplitude of the third maximum of the 0.16-mm sample was measured as a function of temperature. This dependence on temperature is shown in Fig. 10. Making use of an extrapolated value for λ at $T=0$°K, $\lambda_0=5$ mm,[19] and using the extrapolated value of the amplitude at $T=0$°K indicated in Fig. 10, $\lambda(T)$ may be determined. The use of an extrapolated λ_0 was necessary due to lack of complete ρ_{11} data. The result of this manipulation is shown in Fig. 11. The variation of λ with temperature over the liquid-helium range is in close agreement with that found by Grenier *et al.*[19] The computed values of λ in the 3–4°K range are rather insensitive to the choice $\lambda_0=5$ mm. Thus it is clear that $\lambda\approx 1$ mm even at 4°K.

Using $\tau=\lambda/v_F$, and the value $v_F=1.58\times 10^8$ cm/sec,[20] a scale for the relaxation time has been constructed in Fig. 11. It is seen that $\tau\approx 10^{-9}$ sec at liquid-helium temperatures. Noting $H_i=aH_0/\lambda$, where H_i is the saturation field for the lens pocket of electrons, the temperature dependence of this quantity may be estimated. The data are shown in Fig. 12. The value $H_i=78$ G was found by Zebouni *et al.*[13] by a least-squares curve fit of σ_{11} at 1.4°K. Note that Fig. 12 indicates $H_i\approx 30$ G at 1.4°K. This suggests $\lambda_0=5$ mm may be an overestimate of the mean free path at 0°K. Better agreement is obtained for $\lambda_0\approx 2$ mm. The implied weak temperature dependence of λ suggests that impurity scattering is already dominant at 2° or 3°K.

Spark-Cut Surfaces and the Grenier Oscillations

Grenier *et al.*[19] have reported the observation of a set of short-period oscillations superimposed on the long-

period oscillations due to the lens. These oscillations are ascribed to the "hole arms" in the second Brillouin zone. The ratio of the period of the lens oscillations to the Grenier oscillations was 4.3, and the Grenier oscillations were found to be about $\frac{1}{10}$ the amplitude of the lens oscillations (see Ref. 19, Fig. 16). Both sets were insensitive to 10° rotations away from the hexagonal direction.

It had been hoped to find multiple periods in the present data, especially in the thinner samples where the amplitude would be enhanced. However, examination of Fig. 9 shows absolutely no indication of the Grenier oscillations. The small irregularity seen in Fig. 9 on the trailing edge of the first minimum in the 0.09-mm sample is the only distortion observed. This distortion is believed due to the superposition of sinusoids of approximately the same period due to the bad geometry.

It was noticed that Grenier *et al.* used a "slight acid polish" to remove damage produced by the spark machining. It is considered very likely that the present procedure of electropolishing a minimum of 100 μ of surface produced a more perfect surface. Therefore, a second single crystal was cut from the original ingot, properly oriented, and planed to approximately 1.0 mm in thickness. No chemical treatment at all was given this surface. Data were taken on this sample using a variety of magnetic field sweep rates and amplifier adjustments. The lens oscillations were identical to those obtained in the 1.01-mm electropolished sample shown in Fig. 9 except that the amplitude was twice as large in the spark-planed sample. Again, there was no hint of the Grenier oscillations, though the noise level was only 1% of the amplitude of the lens oscillations. The data were insensitive to rotations of the magnetic field up to 15° away from the hexagonal direction.

It is suggested that two competing mechanisms affect the amplitude of the oscillations. The observation of a slight increase in amplitude in the 0.16-mm sample after abrasion with No. 600 SiC paper and the increase in amplitude by a factor of two between the spark-cut and electropolished cases are strong evidence that an appreciable proportion of the electrons are undergoing specular reflection at the crystal surfaces, even though the de Broglie wavelength at the Fermi surface is only about 4.5 Å. The abrasion and, more significantly, spark planing convert an appreciable fraction of these reflections from a specular to a diffuse nature. Thus a somewhat damaged surface may be preferable to a perfect surface for observing size-effect oscillations. However, if the period of the oscillations is short, a large value of n is obtained quickly as H is increased, and the damping effect of the distorted layer becomes significant at relatively low field. Referring to Fig. 9, a tendency is noted in all normal cases for the amplitude of $\tilde{\rho}_{21}$ to grow at low field and then become constant. It is suggested that Grenier *et al.* hit upon that happy situation in which the enhancement due to increased diffuse scattering outweighs the damping factor.

CONCLUSIONS

The preceding experimental data and analyses support the following conclusions concerning the size-effect oscillatory phenomena in cadmium:

(1) The observed oscillations are quasiperiodic in the magnetic field, with period proportional to the reciprocal thickness. This gives a measure of the radius of curvature of the Fermi surface in the hexagonal direction of $k_F=1.37$ Å^{-1}. This value is 2.9% less than the free electron value, and 0.7% greater than the lens value. It is conclusive that the lens-shaped pocket of electrons is responsible for the oscillations.

(2) The observed constancy of $\tilde{\rho}_{21}$ at high magnetic field is confirmation of the H^{-4} damping of $\tilde{\sigma}_{12}$ predicted by the Sondheimer-Grenier theory.

(3) The experimental value of the mean phase is $\delta=0$ whereas theory predicts $\delta=\pi/2$. Thus the phase may not be trusted to give an indication of the sign of the carriers responsible for the oscillations.

(4) The mean free path is in the millimeter range at liquid-helium temperatures. Complete ρ_{11} data plus a study of the temperature dependence of the amplitude of $\tilde{\rho}_{21}$ give a direct measurement of the mean free path as a function of temperature.

(5) In order to observe a number of periods of the order of n, it is necessary that otherwise perfect surfaces be planed parallel to approximately $(1/n)$ times the thickness.

(6) Perfect surfaces, i.e., cleaved or electropolished surfaces, may not be the best choice for the observation of Sondeimer oscillations. In cadmium the scattering is only partially diffuse, and the amplitude may be enhanced by introducing a thin distorted layer. However, this effect may be offset by the damping thereby introduced.

ACKNOWLEDGMENTS

The authors wish to express their appreciation to Dr. C. G. Grenier for valuable comments and in particular for suggesting the viscous-medium model. We are grateful to Dr. M. E. Anderson, Dr. W. D. Deering, and Dr. G. W. Kattawar for helpful discussions. Also, we are indebted to Dr. L. F. Connell for reading the manuscript.